Atmosfera (1997), **10**, *pp. 75-99*

Tropopause-height feedback and radiative forcing in 2D climate simulations

L. DELOBBE,* C. TRICOT, ** and J. P. VAN YPERSELE*

* *Université Catholique de Louvain, Institut d'Astronomie et de Géophysique G. Lemaître, 2 Chemin du Cyclotron, 1348 Louvain-la Neuve, Belgium*

** *Institut Royal Météorologique de Belgique, Département de Climatologie, 3 Avenue Circulaire, 1180 Bruzelles, Belgium*

(Manuscript received April 18, 1996; accepted in final form August 14, 1996)

RESUMEN

Se estudia la respuesta climática del Hemisferio Norte al forzamiento de los gases de invernadero antropogénicos con un modelo climático zonalmente promediado. Primero, se propone un método simple para mejorar el forzamiento radiativo con modelos climáticos de baja resolución vertical de la dinámica atmosférica. Luego, se examina la sensibilidad de la respuesta del modelo a la parametrización de la altitud de la tropopausa. Se demuestra que unos cambios pequeños en la altitud de la tropopausa inducidos por el calentamiento climático inducen una retroalimentación importante que afecta fuertemente la sensibilidad de $2 \times CO_2$ en el equilibrio.

Finalmente, se simula la evolución climática transitoria para los forzamientos radiativos, dependientes del tiempo, correspondientes a los escenarios BaU y D del IPCC 1990. Se toman en cuenta las contribuciones de varios gases de invernadero con un método CO_2-efectivo cuya variabilidad se discute brevemente. Varias simulacions transitorias se llevaron a cabo con diferentes parametrizaciones de la altitud de la tropopausa. Los resultados muestran, asimismo, que la retroalimentación de la altitud potencial de la tropopausa puede influir significativamente en la respuesta del modelo.

ABSTRACT

The climate response of the Northern Hemisphere to the anthropogenic greenhouse gas forcing is studied with a zonally-averaged climate model. First, a simple method is proposed to improve the radiative forcing in climate models with a low vertical resolution for the atmospheric dynamics. Then, the sensitivity of the model response to tropopause height parameterization is examined. It is shown that small changes in tropopause height induced by climate warming introduce an important feedback which strongly affects the $2 \times CO_2$ sensitivity at equilibrium. Finally, transient climate evolution is simulated for the time-dependent radiative forcings corresponding to the scenarios BaU and D of the IPCC 1990. The contributions of various greenhouse gases are taken into account with an effective-CO_2 method whose validity is shortly discussed. Several transient simulations have been undertaken with different tropopause height parameterizations. The results show further that the potential tropopause-height feedback can significantly influence the model response.

1. Introduction

The major part of the solar radiation penetrating the Earth-atmosphere system is absorbed by the Earth surface which, in turn, reemits it upwards as infrared or longwave radiation. Some radiatively active gases present in the atmosphere absorb and emit this longwave radiation but, due to the decrease in tropospheric temperature with increasing height, these gases radiate to space at a colder atmospheric temperature. The net effect is a trapping of longwave energy by the atmosphere, usually referred to as the greenhouse effect. Without this trapping of around 154 Wm^{-2}, the global mean air temperature at the Earth surface would be 33°C lower than the current value of 15°C (e.g., Ramanathan *et al.*, 1987).

The main contributers to the greenhouse effect are water vapour and carbon dioxide but other atmospheric constituents like ozone, methane, nitrous oxide and halocarbons also play an important role. Since the preindustrial era, emissions of greenhouse gases, mainly CO_2, CH_4, N_2O and CFCs, resulting from human activities tend to enhance the natural greenhouse effect, causing an additional warming of the Earth surface.

In order to assess the potential climate changes in the next century, a lot of climate models have been developed. These models can be used to carry out equilibrium experiments that simulate the state of the climate system when it is in balance with the radiative forcing (in the case of a doubling of the CO_2 concentration, for instance). However, because of the thermal capacity of the oceans which delays the climate response to the radiative forcing, our climate is never in equilibrium with the time-dependent radiative forcing induced by the anthropogenic greenhouse effect enhancement. Therefore, transient simulations including the ocean delay effect must be carried out.

In order to perform a rather large number of simulations with a long period of integration, a two-dimensional (altitude-latitude) climate model has been used in the present study. The model, which is described in detail in Gallée *et al.* (1991), is designed for simulating the climate of the Northern Hemisphere. The atmospheric dynamics is represented by the quasigeostrophic approximation. Since it is cruder than the representation with the primitive equations, this approximation allows a 3 day time step integration and, consequently, a higher integration speed. The climate model, coupled to a diffusive ocean (Smits *et al.*, 1993), is used to investigate the transient response of the Northern Hemisphere to the radiative forcing resulting from the increased concentrations of the atmospheric greenhouse gases, at the secular time scale. In the present study, we investigate the sensitivity of the model response to the radiative forcing and to the representation of the tropopause-height feedback. Indeed, this feedback, caused by the elevation of the tropopause with the surface temperature, could strongly influence the sensitivity of climate models. However, current General Circulation Models (GCMs) may not represent accurately this feedback because the tropopause pressure changes are very small compared to the vertical resolution around the tropopause. The aim of our simulations, carried out with a simplified climate model, is to stress the important role that this feedback can play.

The relevant parts of the model used for this study are described in section 2. That description shows that the model is forced by the radiative perturbation at the top of the atmosphere instead of the perturbation at the tropopause. In the same section, a simple way to improve the radiative forcing of the model is proposed and tested. Section 3 is devoted to the analysis of the radiative forcing due to the different greenhouse gases. In order to study the climatic effect of CH_4, N_2O and CFCs which are not explicitly taken into account in the radiative routines of the model, these gases are introduced as an equivalent CO_2 concentration. The validity of this method will be discussed. In section 4, we investigate the influence of the tropopause height parameterization on the model sensitivity. Results of several transient simulations are presented in section 5. Concluding remarks are finally given in Section 6.

2. Model description

2.1 General description

The LLN-2D model is a two-dimensional zonally averaged climate model (latitude, altitude) designed for simulating the seasonal cycle of the climate of the Northern Hemisphere (Gallée *et al.*, 1991 and 1992). It has a latitudinal resolution of 5^o. In each latitudinal belt the surface is divided into at most five oceanic or continental surface types, each of which interacts separately with the subsurface and the atmosphere. The surface types are ice-free ocean, sea ice, snow-covered and snow-free land, and the Greenland ice sheet, which is allowed to extend from 60°N to 85°N.

The atmospheric dynamics is represented by an improved zonally averaged quasi-geostrophic model. The zonal wind is computed at 250 hPa and 750 hPa, and the atmospheric temperature at 500 hPa (Fig. 1). The model includes a parameterization of the meridional transport of quasi-geostrophic potential vorticity and a parameterization of the Hadley meridional sensible heat transport. Precipitation, vertical radiative (solar and infrared) and turbulent (sensible and latent) heat fluxes, and surface friction are also represented and provide a coupling between the atmosphere and the surface.

Separate energy balances are calculated over the various surface types at each latitude. At the top of the model, solar and IR fluxes contribute to the net energy flux available to the system. The heating of the atmosphere due to the vertical heat fluxes is the weighted average of the convergence of these fluxes above each kind of surface. The other surface and subsurface parameters and processes which are represented are the albedo of each surface type, the oceanic heat transport, the oceanic mixed-layer dynamics, the sea-ice budget, and the surface water availability. In particular, the soil water budget of snow-free land is simulated and influences the surface albedo. Explicit snow budgets are computed for land and the Greenland ice sheet, depending on snowfall and snowmelt. The fraction of snow cover can vary over land and is assumed equal to unity over the ice sheet. The snow albedo is allowed to depend on the snow age, the snow surface temperature, and the solar elevation angle.

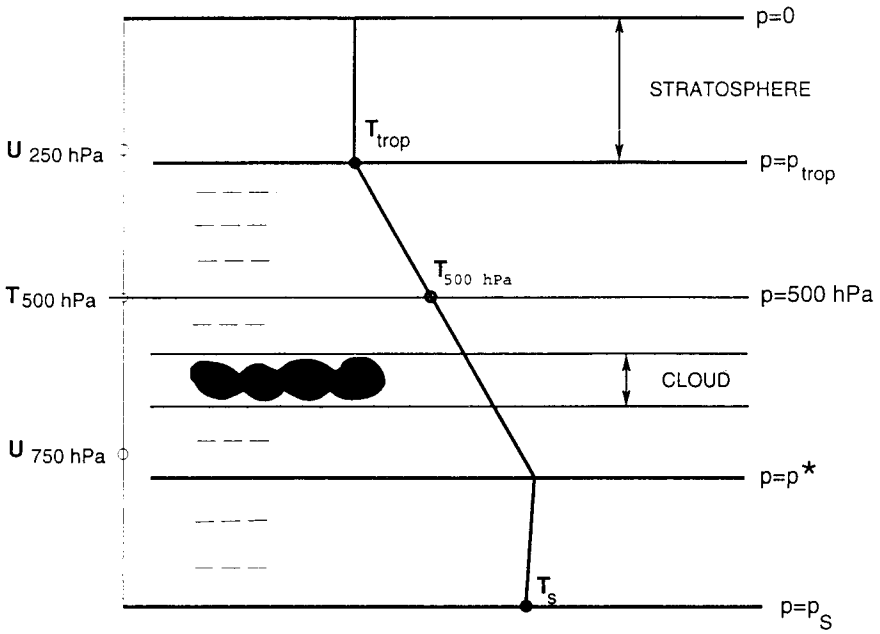

Fig. 1. Temperature profile and vertical discretization in the atmospheric representation of LLN-2D model.

The upper-ocean model is represented by the variable depth and temperature mixed-layer model. In order to simulate the oceanic heat transport and its influence upon the sea surface temperature, a diffusive parameterization of meridional convergence of heat has been included in the model. The model is coupled to a diffusive ocean in which the uptake of heat perturbations by the deep ocean was approximated as a vertical diffusion process as in Smits *et al.* (1993). The model time step is 3 days, except for the mixed-layer and sea ice computations, for which it is 1 day. The model conserves energy within 10^{-4} Wm^{-2} on the hemispheric and annual average (Gallée *et al.*, 1991).

The calculation of the radiative fluxes requires a knowledge of the vertical temperature profile and the vertical distribution of the main optically active atmospheric constituents above the different surface types. Given the model-predicted zonally averaged temperature at 500 hPa, the vertical temperature profile in the troposphere is determined by assuming that the product of the static stability parameter and the pressure p is constant throughout that layer. The vertical resolution for the radiative computations is around 100 hPa in the troposphere. One layer corresponds to the stratosphere.

The temperature profile under a specified pressure level (p^*) is linearly modified so that the air near the surface has the same temperature as the surface (Fig. 1). Such correction is necessary to allow, for example, thermal inversion over cold surfaces. The stratosphere is supposed isothermal with a temperature identical to that of the tropopause. Tropopause pressure is parameterized as a function of the zonally averaged surface temperature after Sellers (1983)(see section 4).

The vertical variation of specific humidity is deduced from the zonally averaged surface temperature and relative humidity according to the formulation of Smith (1966) adapted from the monthly and zonally averaged humidity profile given by Oort (1983). Mean annual climatological values of relative humidity are used separately over continental and oceanic surfaces. The CO_2 concentration is homogeneous in the atmosphere.

The total ozone amount is parameterized as a function of latitude and time following Van Heuklon (1979) and the vertical profiles are given by the formulation of Lacis and Hansen (1974).

Three kinds of aerosols are considered: continental, maritime and unperturbed stratospheric. Their vertical profiles and radiatives parameters are taken from WCP (1986).

An effective single cloud is assumed to exist in each latitude belt, with annual mean cloud amounts deduced from London's (1957) data (Ohring and Adler, 1978) and supposed to be equal over each surface type. Monthly variations of the zonal cloudiness are introduced by superposing a seasonal cycle on the annual mean values following the monthly mean data of Berlyand and Strokina (1980). The base and top altitudes of the cloud layer and its optical thickness are kept fixed throughout the year following Chou *et al.* (1981).

The seasonal cycle of the incoming solar radiation at the top of the atmosphere is computed as a function of the latitude, the semi-major axis of the ecliptic, its excentricity, its obliquity and the longitude of the perihelion, following Berger (1978). The solar radiation scheme used here has been developed from the one described by Fouquart and Bonnel (1980). The following processes are included : absorption by H_2O, CO_2, and O_3, Rayleigh scattering, absorption and scattering by cloud droplets and aerosols, and reflection by the Earth's surface. The longwave radiation computations are based on Morcrette's (1984) wideband formulation of the radiative transfer equation. Absorption by H_2O, CO_2, and O_3 is explicitly treated and the cloud cover is supposed to behave as a blackbody, as is the Earth's surface. In both schemes, account is taken of variations in surface topography.

2.2 Improvement of the radiative forcing

As mentioned above, the radiative contribution to the diabatic heating of the atmosphere is given by the convergence of the solar and infrared radiative fluxes between the surface and the top of the atmosphere. Our model is thus forced by the radiative perturbation at the top of the atmosphere (TOA) and not at the tropopause, as it should be. The Earth's surface and the troposphere are indeed tightly coupled via air motions and, therefore, they must be considered as a single thermodynamic system (Ramanathan *et al.*, 1987). In a first approximation, the stratosphere can be considered in radiative equilibrium without exchange of latent and sensible heat with the troposphere. As a result, the radiative forcing of the climate system is the change in radiative flux at the tropopause.

Forcing the model with the radiative perturbations at the TOA leads to an underestimation of the infrared forcing since these perturbations are lower than the tropopause perturbations. Figures 2 and 3 show the seasonal and latitudinal distributions of the radiative perturbation computed respectively at the tropopause and at the TOA, for a doubling of the CO_2 concentration. The annual hemispherical mean values are respectively -4.57 and -3.06 Wm^{-2} at the tropopause and at the TOA. The negative sign means a decrease in upward infrared net flux. The 2 × CO_2 radiative forcing which is obtained at the tropopause is very close to the tropopause radiative forcing calculated with more detailed radiative models. As will be seen later (section 3, Table 1), this forcing is estimated at -5.04 Wm^{-2} after Rind and Lacis (1993), -4.34 Wm^{-2} after Kratz *et al.* (1993) and -5.2 Wm^{-2} after Briegleb (1992). These results show that the vertical resolution of the radiative calculations allows to evaluate accurately the radiative perturbation at the tropopause.

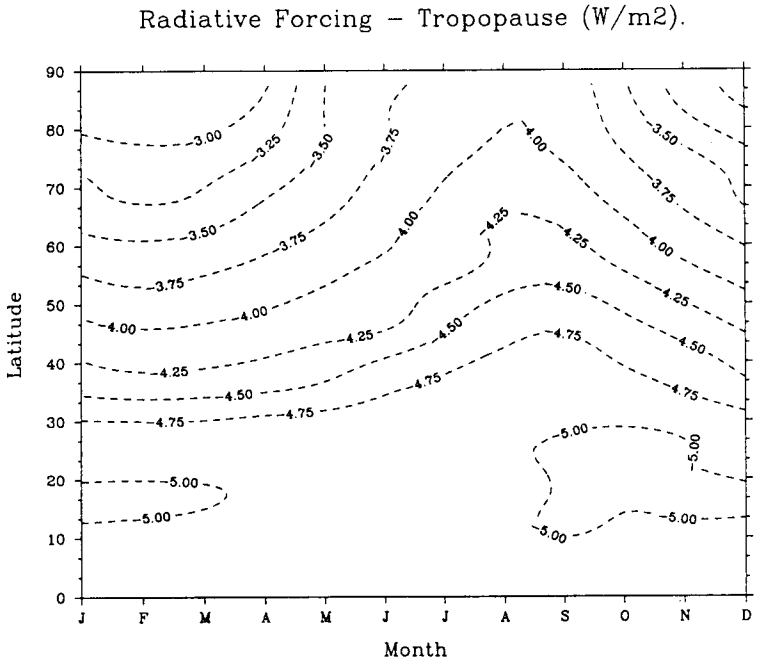

Fig. 2. Latitudinal and seasonal distribution of the tropopause radiative forcing for a CO_2 doubling as computed by the model.

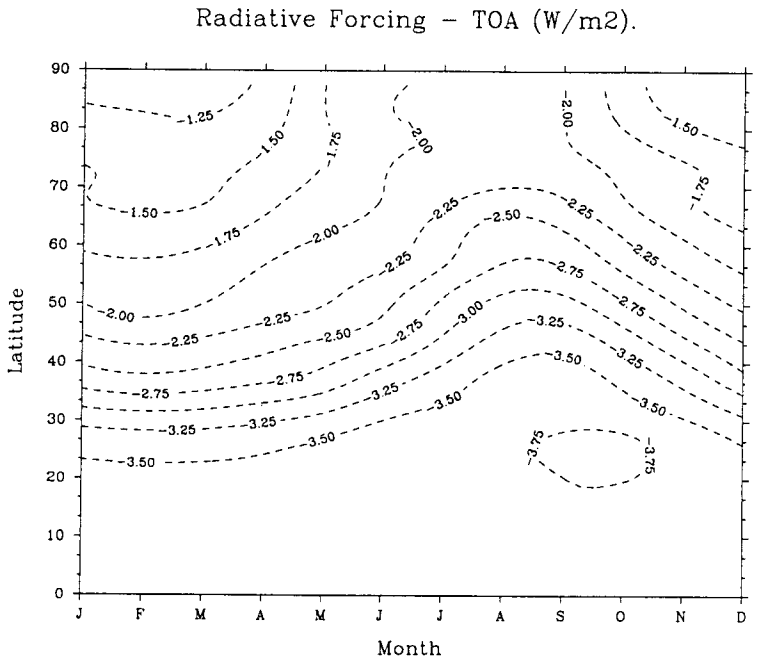

Fig. 3. Latitudinal and seasonal distribution of the TOA radiative forcing for a CO_2 doubling as computed by the model.

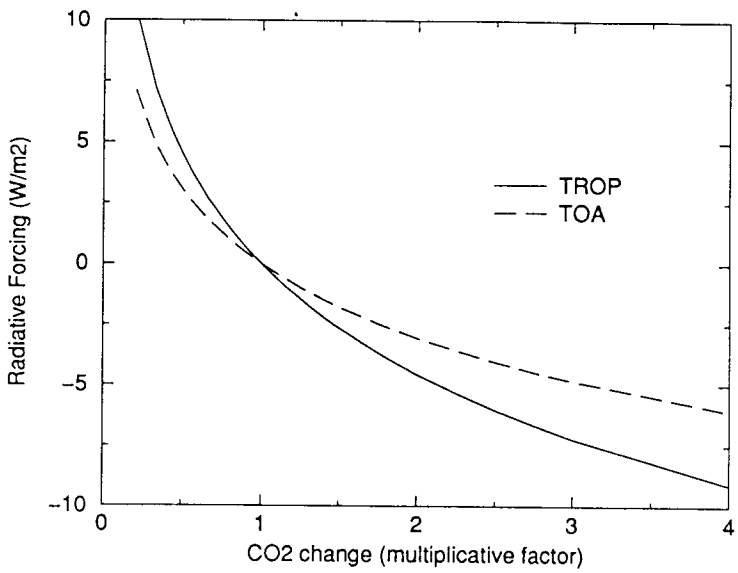

Fig. 4. Radiative forcing, at the tropopause and at the TOA, in annual and hemispherical mean, as a function of the CO_2 change (CO_2 / CO_2^0).

Therefore, an easy way to improve the radiative forcing in our model consists in using a corrected CO_2 concentration such that the radiative perturbation induced at the TOA by the variation of this corrected CO_2 concentration is equal to that induced at the tropopause by the real CO_2 variation. In order to establish this corrected CO_2, the radiative perturbations must be parameterized as a function of the CO_2 variations. We ran the LLN-2D model to equilibrium for present CO_2 concentration (330 ppmv) and then used the radiative routines of the model to evaluate the upward net flux variations, in annual and hemispherical means, at the tropopause and at the TOA, for 26 different CO_2 perturbations extending from 0.2 $\times$ CO_2 to 4 $\times$ CO_2. As shown in Figure 4, it appears that these radiative perturbations can be approximated by a logarithmic function of the CO_2 variations. The least square regressions for the radiative forcing at the tropopause and at the TOA are given by the following expressions:

$$\triangle F_{TROP}(CO_2) = a_1 \ln(\frac{CO_2}{CO_2^0}) \tag{1}$$

$$\triangle F_{TOA}(CO_2) = a_2 \ln(\frac{CO_2}{CO_2^0}) \tag{2}$$

where CO_2^o is the initial CO_2 concentration, CO_2 is the modified concentration, a_1= -6.54 and a_2= -4.41.

It is worth noting that the expression of the radiative forcing at the tropopause obtained with our model is quite similar to the expression given in the IPCC (1990) report :

$$\triangle F_{TROP}(CO_2) = -6.3 \ln(\frac{CO_2}{CO_2^0}) \tag{3}$$

The corrected CO_2 concentration is then defined by:

$$\triangle F_{TOA}(CO_2^{corr}) = \triangle F_{TROP}(CO_2) \tag{4}$$

By introducing (1) and (2) in this definition, the following expression for the corrected CO_2 is obtained:

$$CO_2^{corr} = CO_2^0 (\frac{CO_2}{CO_2^0})^{\frac{a_1}{a_2}} \tag{5}$$

where a_1/a_2=1.48

For a doubling of the real CO_2 concentration, the change of CO_2^{corr} that must be applied to the model is 2.79 $\times$ CO_2^0 . For a 0.5 $\times$ CO_2^0, the corresponding CO_2^{corr} perturbation is 0.36 $\times$ CO_2^0. Using this method affects strongly the model sensitivity to greenhouse gas changes. The global mean temperature change for a 2 $\times$ CO_2 experiment goes up from 1.9 K to 3 K when this improvement is introduced.

The regression coefficients of the logarithmic functions (1) and (2) have been evaluated for CO_2 induced climate perturbations with respect to the present climate whose CO_2 concentration is fixed at 330 ppmv. These parameterizations are not necessarily valid for climates significantly different from the current one. However, within the framework of paleoclimate reconstructions which have been carried out with a new two-hemispherical version of the model, we have also

evaluated the coefficients a_1 and a_2 for 122 climate states distributed in a time period extending from 122 000 years before present to now. Results of simulations show that the regression coefficients vary very little along this period (between -6.26 and -6.54 for a_1, and between -4.44 and -4.18 for a_2). In particular, the ratio of a_1 to a_2, which is used in (5), is always comprised between 1.47 and 1.49. Thus, the expression (5) giving the corrected CO_2 concentration is almost independent of the climate state and remains valid for use in the LLN-2D model whatever the climate may be.

3. Radiative forcing of climate

Carbon dioxide is not the only greenhouse gas. Over the period extending from 1765 to 1990, the estimated contributions of the different anthropogenic greenhouse gases to the total radiative forcing are 61% for CO_2, 23% for CH_4, 4% for N_2O and 12% for the CFCs (IPCC, 1990). It must be noted that 26% of the radiative effect of methane result from the increase in stratospheric water vapor concentrations due to methane oxidation (IPCC, 1992). These radiative forcing values are the values which would be obtained if the greenhouse gas concentrations went up instantaneously from their 1765 preindustrial values to their estimated values in 1990. In 1990, the total radiative forcing with respect to 1765 is evaluated to 2.45 Wm^{-2} with 61% due to CO_2. These figures stress the importance of accurately taking into account the role of greenhouse gases other than CO_2. In the future, the effect of these gases will probably remain significant.

An easy way to include the effect of greenhouse gases other than CO_2 consists in introducing them as an effective CO_2 concentration such that radiative perturbations induced by the effective CO_2 and by the totality of the greenhouse gases are equal (Tricot and Berger, 1987). By using detailed radiative models, it is possible to establish approached analytical expressions relating, for each greenhouse gas, the radiative forcing to the concentration change. We have used the expressions given in IPCC (1990) report, for the main gases (i.e. CH_4, N_2O, CFC11 and CFC12). Such expressions are difficult to establish for ozone because its radiative effect is highly dependent on the vertical concentration profile (Ramanathan *et al.*, 1985). We will therefore ignore the changes of ozone concentration in our simulations.

Knowing the concentration changes for the different greenhouse gases with respect to a reference year, the total radiative forcing $\triangle F_{tot}$ is obtained by adding the contributions of each gas. The effective CO_2 concentration is then evaluated by using the IPCC (1990) expression of the radiative forcing for CO_2 :

$$CO_2^{eff} = CO_2^0 \exp(\frac{\triangle F_{tot}}{6.3}) \tag{6}$$

where CO_2^0 is the CO_2 concentration in the reference year.

We have evaluated the effective CO_2 concentrations associated to scenarios BaU (Business-as-Usual) and D (Accelerated policies) of the IPCC (1990). Both scenarios give the concentrations of the greenhouse gases until 2100. The former (BaU) forecasts emissions which are allowed to increase unrestricted whereas the latter (D) supposes severe emission reductions. The effective CO_2 concentrations have been evaluated for both scenarios with respect to the year 1850. For that year, the effective CO_2 is then equal to the CO_2 concentration alone (288 ppmv). Figures 5 and 6 show the results obtained by considering both the joint effect of all greenhouse gases and their individual effect.

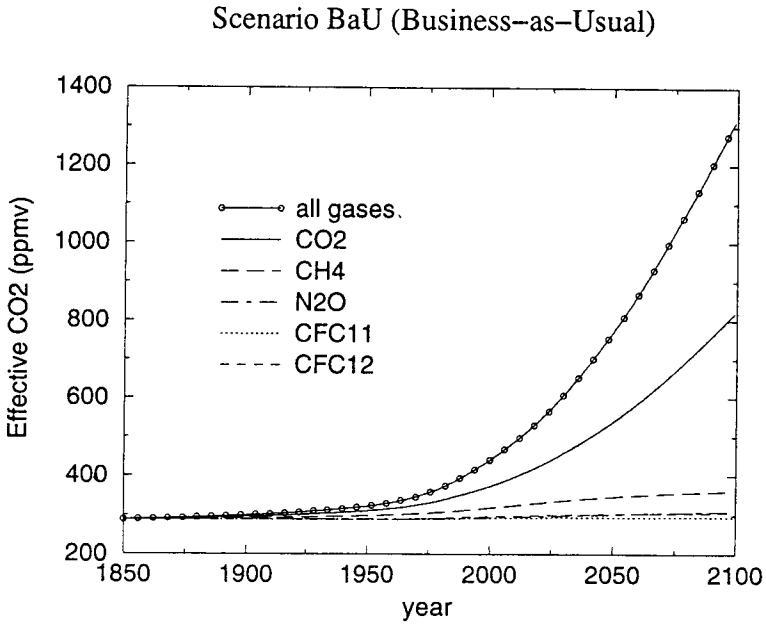

Fig. 5. Effective CO_2 changes for scenario BaU.

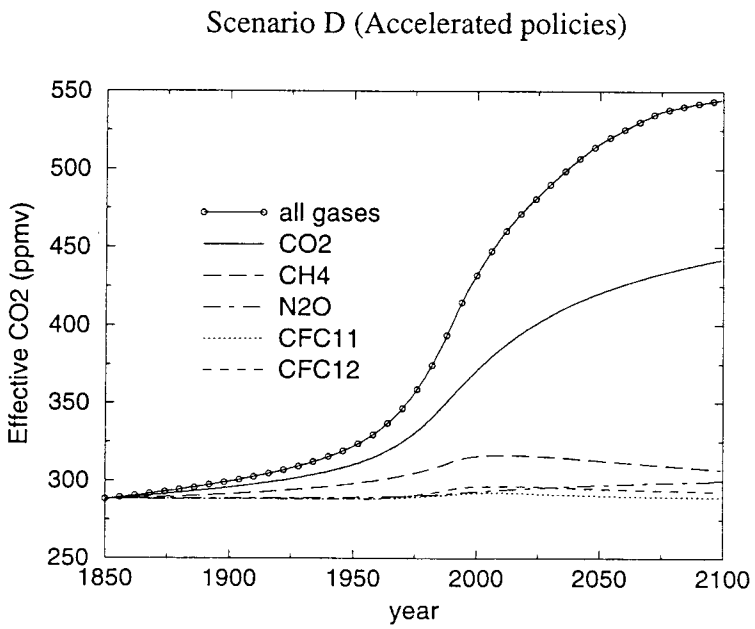

Fig. 6. Effective CO_2 changes for scenario D.

This effective CO_2 method is a possible way to simulate the effect of greenhouse gases other then CO_2 in climate models whose radiative routines do not explicitly take these gases into account. However, the vertical distribution of the radiative forcing for CO_2 is different from that of the other trace gases (Wang *et al.*, 1991). Since the vertical absorption and heating rate

profiles are different for each gas, the dependence of these profiles on atmospheric characteristics like cloudiness, temperature or water vapor will also be different. Consequently, concentrations changes of trace gases other than CO_2 will produce radiative forcings and surface heatings whose regional pattern will not be similar.

The effective CO_2 method would then not allow to properly simulate the spatial variations of radiative forcing and resulting temperature changes. By using an atmospheric general circulation model, Wang *et al.* (1992) have simulated, on the one hand, the current equilibrium climate and on the other hand, the equilibrium climate associated with the trace gas concentrations given in 2050 by the BaU scenario. Two types of experiment have been carried out: the first includes CO_2 and other trace gases explicitly and the second uses an effective CO_2. The comparison of the surface temperature changes shows that, in some areas, the estimated warming error made by using an effective CO_2 could reach 20 %. Nevertheless, in global mean, the results obtained on the one hand with an effective CO_2 and, on the other hand, with an explicit treatment of all the trace gases, are almost identical: the global warmings are respectively evaluated to 3.8 and 3.9 K. For the model LLN-2D, whose aim is neither to reproduce accurately the regional distribution of the temperature changes neither to simulate precisely the vertical temperature profile, the use of this method seems thus justified.

Moreover, the values of radiative forcing at the tropopause obtained with our model by using the effective CO_2 method are in good agreement with those obtained with radiative models that take explicitly into account the different greenhouse gases. First we have evaluated the effective CO_2 changes corresponding to individual gas changes such as $2 \times CH_4$ or $2 \times N_2O$. Figure 7 shows the variations of effective CO_2 as a function of the variation of the different greenhouse gases. The values obtained for some particular concentration changes are presented in Table 1. For each of these values, radiative forcing at the tropopause, in hemispherical and annual mean, has been calculated with our model whitout using the correction described in section 2.2. Results are given in Table 1 together with values obtained with radiative models which resolve explicitly the absorption by CO_2, CH_4, N_2O, CFC11 and CFC12 (Rind and Lacis, 1993; Briegleb, 1992; Kratz *et al.*, 1993). The comparison of these results confirms that the use of an effective CO_2 is quite valid in our 2D model.

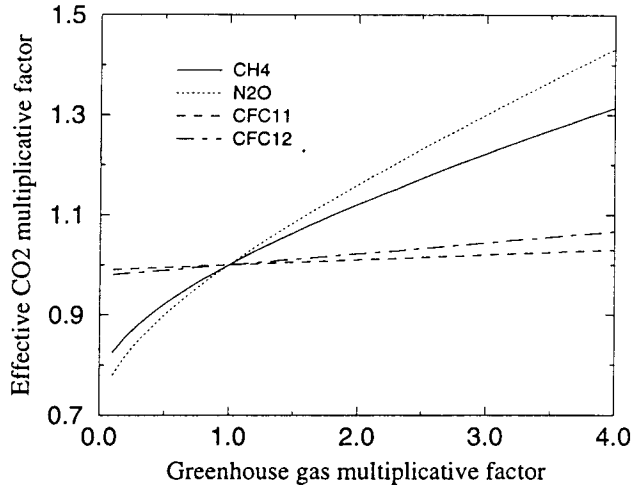

Fig. 7. Effective CO_2 variations CO_2^{eff} / CO_2^0 as a function of the variation of the different gases.

Table 1. Tropopause radiative forcing (Wm^{-2}) induced by greenhouse gas concentration changes. Comparison between results obtained with LLN-2D and with other radiative models (Rind and Lacis, 1993; Kratz *et al.*, 1993; Briegleb, 1992).

× GHG	$\frac{CO_2^{eff}}{CO_2^0}$	ΔF_{TROP} (LLN-2D)	ΔF_{TROP} (Rind)	ΔF_{TROP} (Kratz)	ΔF_{TROP} (Briegleb)
0.5 × CO_2	0.5	4.54			
2 × CO_2	2	-4.57	-5.04	-4.34	-5.2
4 × CO_2	4	-9.09			- 10.4
0.2 × CH_4	0.86	1.03			
2 × CH_4	1.12	-0.76	-0.53	-0.61	-0.8
4 × CH_4	1.32	-1.83			-1.87
0.5 × N_2O	0.90	0.66			
2 × N_2O	1.15	-0.93	-0.95	-0.89	-1.04
4 × N_2O	1.41	-2.25			-2.34
0 - 1 ppbv CFC11	1.036	-0.23	-0.21	-0.22	
0 - 1 ppbv CFC12	1.045	- 0.29	-0.26	-0.28	

4. Sensitivity to tropopause pressure

The sensitivity of the standard version of LLN-2D model for a CO_2 doubling is 3 K (with the correction described in section 2.2). However, there is still a large dispersion in the sensitivities of current global climate models. In particular, the way of representing cloud-climate feedbacks introduces a threefold variation in climate sensitivity (Cess *et al.*, 1990). Besides, other parameterizations used in climate models (in radiative schemes for instance), can also significantly affect the model sensitivities. Here, we study the influence of the tropopause pressure parameterization in the model. In the standard version of LLN-2D model, the tropopause pressure (p_{trop}) is parameterized as a function of the surface temperature in zonal mean (T_s), following Sellers (1983) :

$$p_{trop}(hPa) = 200 - 110 \tanh\left(0.05(T_s(K) - 285)\right) \quad (7)$$

This relationship expresses an elevation of the tropopause with the surface temperature which introduces a positive feedback in the model. The stratospheric temperature being supposed equal to that of the tropopause, a tropopause elevation leads to a cooling of the whole stratospheric column. This cooling induces a reduction of the upward infrared flux at the top of the atmos-

phere which must be compensated by an increase of the surface temperature. This simplified parameterization is based on present day climate observations only and may not be a good representation of the real processes which determine the change of the tropopause height in a warming climate.

Table 2. Simulated global mean surface temperature (Ts) obtained with different tropopause parameterizations.

p_{trop} (hPa)	T_s (K)	p_{trop} (hPa)	T_s (K)
250	283.4	Sellers	288.0
200	286.8	Rennick	282.2
190	287.5	Rennick - 50 hPa	286.9
180	288.0	Rennick -65 hPa	288.1

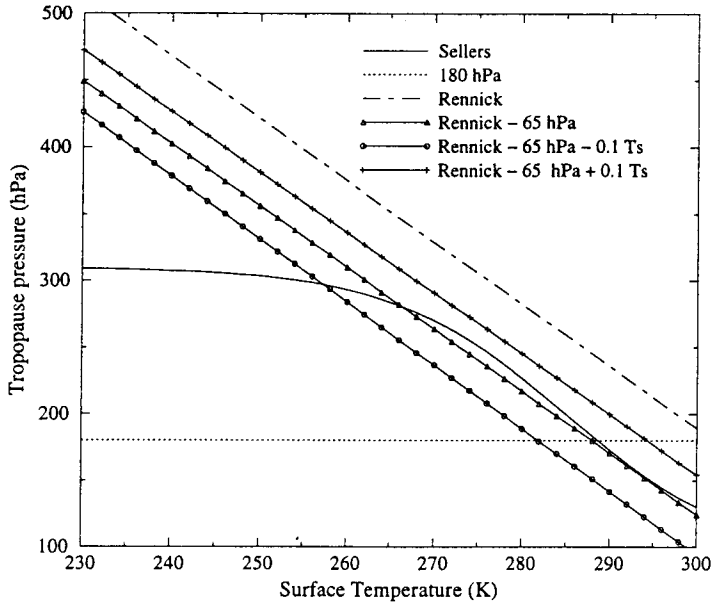

Fig. 8. Tropopause pressure as a function of the surface temperature for different tropopause pressure parameterizations.

Several tropopause pressure parameterizations have been tested in order to assess the influence on the 2 × CO_2 model sensitivity (Fig. 8). First, we have evaluated the effect on the present climate equilibrium (Table 2). Four experiments have been carried out with fixed tropopause pressures ranging from 180 hPa to 250 hPa. Besides the parameterization proposed by Sellers (1983), we have also used another parameterization based on the zonal mean surface temperature (T_s), which has been proposed by Rennick (1977) :

$$p_{trop}(hPa) = 1581.35 - 4.64T_s(K) \tag{8}$$

Compared with the values of pressure given by the Sellers parameterization, the tropopause pressures obtained by the above expression are too high (see Fig. 8) and lead to global mean surface temperature of 282 K well below the observed value of 288 K. A constant value of 65 hPa must be substracted from (8) to obtain a present climate close to the one obtained by using the Sellers parameterization or by using a constant value of 180 hPa. For present climate, the comparison between these three experiments (denoted A1, A2 and A3 in Table 3) shows that the latitudinal and seasonal distribution of surface temperatures are quite similar. Figure 9 shows, as a function of latitude, the annual mean of the surface temperature, the tropopause pressure and the tropopause temperature for the three experiments. Using a fixed tropopause pressure of 180 hPa (A2) leads to an increase of the surface temperatures of about 2 K in the high latitudes and a decrease in the tropical regions of about 1 K with respect to the two other experiments. The three parameterizations cause large differences in tropopause pressures and, therefore, in tropopause temperatures. Unlike the observations, a tropical tropopause warmer than the polar one is obtained by considering a fixed tropopause pressure. However, as shown in Table 3, the global mean of tropopause pressures and temperatures are quite similar. The seasonal cycles of snow and ice area are also in good agreement, except for the ice area in the end of the summer which is smaller in experiment A2 (Fig. 10).

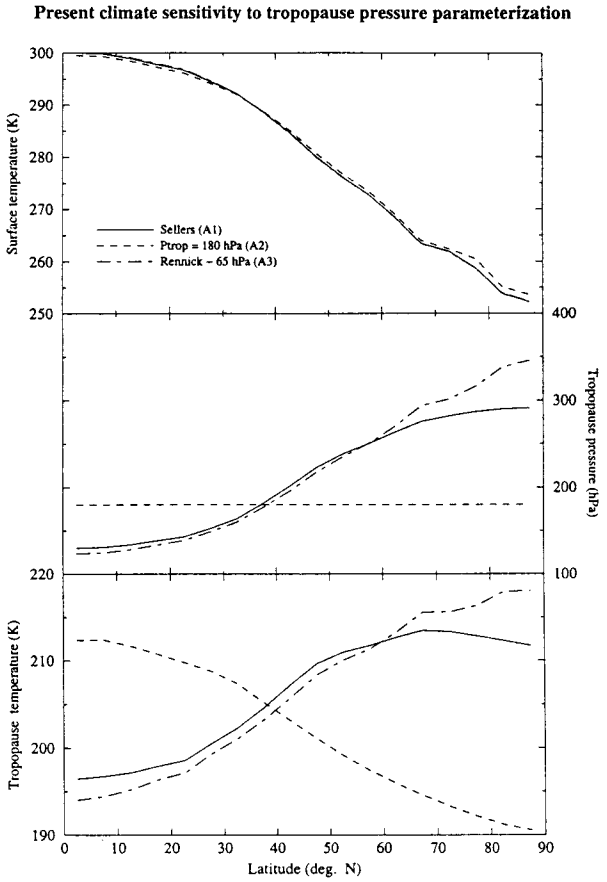

Fig. 9. Present climate simulations : experiments A1, A2 and A3 (see Table 3). Latitudinal distribution of the surface temperature, tropopause pressure and tropopause temperature, in zonal and annual mean.

Table 3. Present climate experiments A1, A2 and A3. Global mean values of surface temperature (T_s), temperature at 500 hPa ($T_{500\ hPa}$), tropopause pressure (p_{trop}), tropopause temperature (T_{trop}) and 2 × CO_2 radiative forcing at the tropopause (ΔF_{trop}) and at the TOA (ΔF_{TOA}).

Experiment	T_s (K)	$T_{500\ hPa}$ (K)	p_{trop} (hPa)	T_{trop} (K)	ΔF_{trop} (W/m^2)	ΔF_{TOA} (W/m^2)
A1. Sellers	288.03	256.6	181	203.3	4.56	3.06
A2. p_{trop} = 180 hPa	288.00	256.5	180	205.7	4.56	2.97
A3. Renn. - 65 hPa	288.08	256.7	180	202.3	4.57	3.10

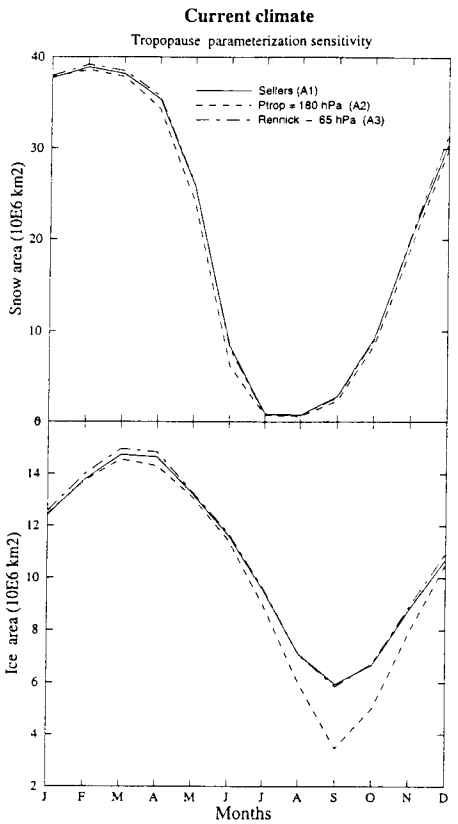

Fig. 10. Seasonal cycles of snow and ice areas for experiments A1, A2 and A3.

Starting from the three simulated present equilibrium climates (A1, A2 and A3), several 2 × CO_2 experiments have been performed. All the results are presented in Table 4 and Figure 11. The CO_2 correction described in section 2.2 is valid for the three parameterizations since they produce the same global mean radiative forcings at the TOA and the tropopause, as given in Table 3 . Therefore, a CO_2 concentration of 921 ppmv has been used in all these experiments. Figure 12 displays the latitudinal distribution of the tropopause radiative forcing in annual mean.

Table 4. CO_2 doubling experiments : global mean values and changes of surface temperature (T_s), temperature at 500 hPa ($T_{500\ hPa}$), tropopause pressure (p_{trop}) and tropopause temperature (T_{trop}). The changes are considered with respect to experiments presented in Table 3 : experiment A1 for experiments B10 and B11, experiment A2 for B20 and experiment A3 for B30, B31 and B32 (see text for description of the experiments).

Experiment	T_s (K)	$T_{500\ hPa}$ (K)	p_{trop} (hPa)	T_{trop} (K)
B10: Sellers w/ f.b.	290.98 (+ 3.0)	259.41 (+ 2.8)	171 (- 10)	202.3 (- 1)
B11: Sellers w/o f.b.	290.29 (+ 2.3)	258.76 (+ 2.1)	181 (+ 0)	204.9 (+ 1.6)
B20: p_{trop}=180 hPa	290.37 (+ 2.4)	258.70 (+ 2.2)	180 (+ 0)	207.3 (+ 1.6)
B30: Rennick (9)	291.40 (+ 3.3)	259.86 (+ 3.2)	164 (- 16)	199.9 (- 2.4)
B31: Rennick (10)	293.58 (+ 5.5)	262.12 (+ 5.4)	125 (- 55)	186.3 (- 18)
B32: Rennick (11)	288.66 (+ 0.6)	257.18 (+ 0.5)	206 (+ 26)	210.1 (+ 7.8)

In the first 2 × CO_2 experiment (B10), the parameterization of Sellers (1983) is used, which introduces a positive feedback due to the tropopause height elevation. If we suppress this feedback (experiment B11) by fixing the tropopause pressure, for each latitude and each moment of the year, to the current value evaluated in the experiment A1, the model sensitivity is significantly modified. The global surface temperature change for a CO_2 doubling goes down from 3 K to 2.3 K. The values of global mean surface temperature, temperature at 500 hPa, tropopause pressure and tropopause temperatures are gathered in Table 4. The experiment B10 shows that a CO_2 doubling leads to a decrease of the tropopause pressure of about 10 hPa and, consequently, to a tropopause temperature decrease of about 1 K, even if the surface temperature increases by 3 K. On the other hand, keeping the tropopause pressures to the current values leads to a 1.6 K warming of the tropopause (exp. B11). In all experiments, the temperature changes at 500 hPa are similar to the surface temperature changes.

Starting from experiment A2, a CO_2 doubling with a tropopause pressure fixed to 180 hPa and, therefore, whithout tropopause feedback (experiment B20), implies a global surface warming of 2.4 K. Through the dependence of the tropopause pressure on the surface temperature, the Rennick parameterization also includes a positive feedback. In order to stress the importance of that feedback, three different tropopause parameterizations (Fig. 8) derived from Rennick (1977) have been used :

$$p_{trop}(hPa) = 1581.35 - 4.64\ T_s(K) - 65 \tag{9}$$

$$p_{trop}(hPa) = 1581.35 - 4.64\ T_s(K) - 65 - 0.1\ T_s(K) \tag{10}$$

$$p_{trop}(hPa) = 1581.35 - 4.64\ T_s(K) - 65 + 0.1\ T_s(K) \tag{11}$$

Expressions (9), (10), (11) correspond respectively to CO_2 doubling experiments B30, B31 and B32. In B31, the tropopause feedback is strengthened whereas it is reduced in experiment B32.

Figure 11 shows that these different tropopause parameterizations strongly influence the climate model sensitivity. Note that, for these three experiments, all the changes are considered with respect to experiment A3 in which the tropopause pressure is determined for present climate according to (9). Experiments B30, B31 and B32 give 2 × CO_2 sensitivities respectively of 3.3 K, 5.5 K and 0.6 K. In this last experiment, Table 4 shows that the tropopause pressure increases with respect to experiment A3. The expression (11) introduces, actually, a large negative tropopause feedback while expression (10) causes a large positive feedback. These two extreme cases show that the representation of the tropopause feedback strongly affects the sensitivity of a climate model. By using a one-dimensional radiative convective atmospheric model with a variable vertical resolution, Sinha and Shine (1994) obtained a tropopause pressure change of around 10 hPa in a 2 × CO_2 experiment, very similar to the value we obtain using the parameterization proposed by Sellers (1983). The vertical resolution of current Global Circulation Models, which is at least 50 hPa, may not be sufficient to represent accurately these tropopause position changes. Besides, the tropopause position influences cirrus height and, therefore, affects also the cloud feedback. In conclusion, the tropopause height changes may prove to be an important feedback in the climate system.

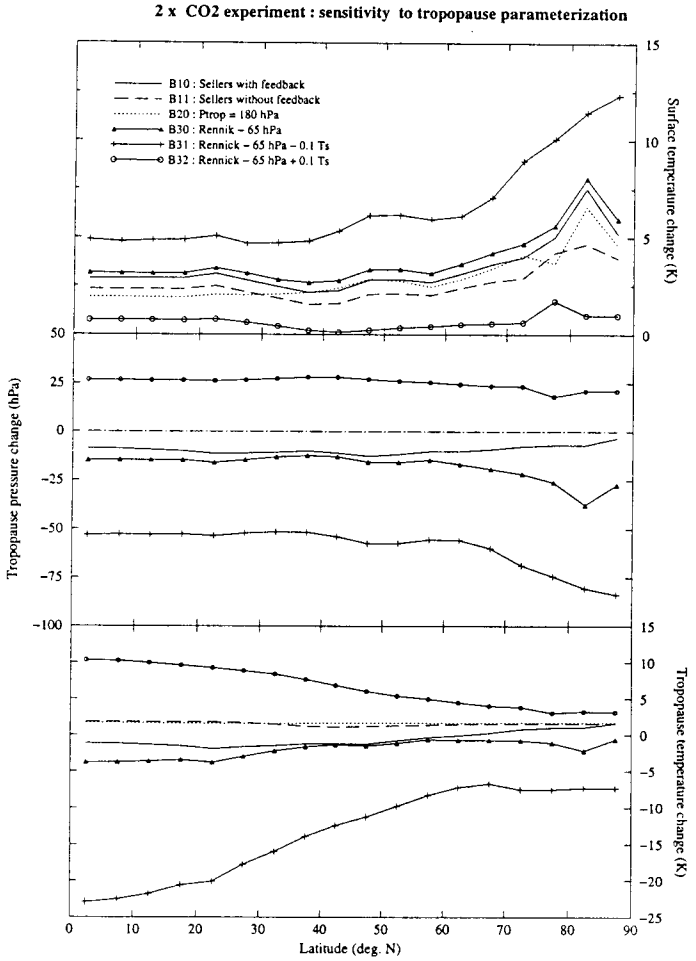

Fig. 11. CO_2 doubling experiments : latitudinal distribution of the changes in surface temperature, tropopause pressure and tropopause temperature for the different tropopause parameterizations. The changes are considered with respect to experiment A1 for experiments B10 and B11, to A2 for B20 and to A3 for B30, B31 and B32 (see Table 4).

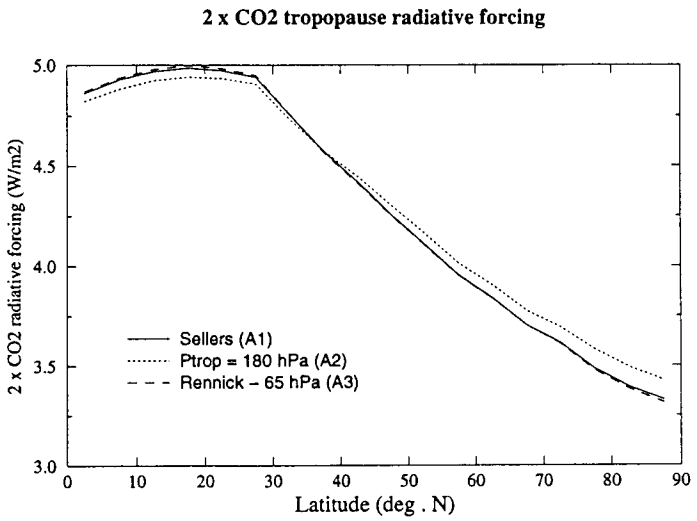

Fig. 12. Radiative forcing : latitudinal distribution of the 2 × CO_2 radiative perturbation induced at the tropopause by an instantaneous CO_2 concentration change from 330 to 660 ppmv.

5. Transient simulations

Thanks to the low computing cost, it has been possible to carry out simulations over a long integration period (250 years) and for a large number of time-dependent radiative forcings. Starting from arbitrary conditions, the model is first run, until an equilibrium seasonal cycle is reached, with gas concentrations equal to those of 1850 and without a diffusive deep ocean. The equilibrium is considered to be achieved when the annual hemispheric mean radiative balance at the top of the atmosphere becomes less than 0.01 Wm^{-2}. A 100 year integration is sufficient to obtain this condition. Using this solution as initial condition, the model is then integrated from 1850 to 2100 allowing heat uptake by vertical oceanic diffusion. The radiative forcing is expressed by the changes in effective CO_2 concentrations. All the effective CO_2 evolutions shown in Figures 5 and 6 have been considered in order to assess the respective contribution of the different greenhouse gases in the anthropogenic climate change. The effective CO_2 values are corrected as described in section 2.2. Tropopause pressure is parameterized following Sellers (1983). Climate responses expressed in terms of surface temperature changes in annual and hemispherical mean are presented in Figures 13 and 14. When all the greenhouse gases are taken into account, the global warmings between 1990 and 2100 are respectively 4.1 and 1.3 K for scenarios BaU and D. The latitudinal and seasonal distributions of temperature change between 1990 and 2050, for both scenarios, are presented in Figures 15 and 16. An important feature is the amplification of the warming in the polar regions during the winter resulting from the temperature-albedo feedback (Colman *et al.*, 1994). As a consequence of global warming, melting of snow and ice tend to be amplified causing a positive feedback in the climate system.

The respective effects of the radiative forcing correction (section 2.2) and of the use of an effective CO_2 concentration are shown in Figures 17 and 18. For both scenarios, the transient temperature evolution is given for four different time-dependent forcings : (a) using the radiative forcing (r.f.) correction and an effective CO_2 concentration that takes into account all the greenhouse gases; (b) using the r.f. correction but taking into account CO_2 alone; (c) without r.f. correction but with all greenhouse gases taken into account; (d) without r.f. correction and with CO_2 alone. Results show that the radiative forcing correction and the introduction of the greenhouse gases other than CO_2 produce effects of the same order of magnitude.

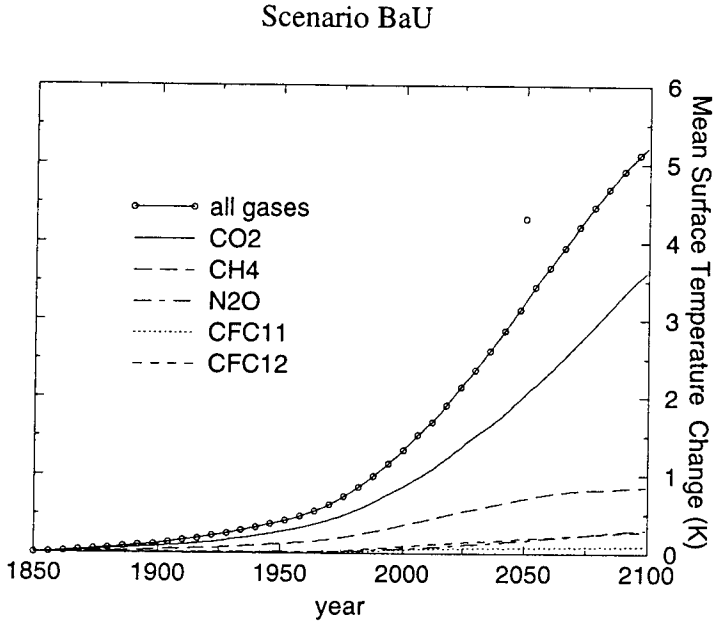

Fig. 13. Transient climate response to greenhouse gas concentration changes expressed in term of mean temperature change from 1850 (T_{1850}=287.5 K). Scenario BaU. The isolated little circle indicates the equilibrium response in 2050 .

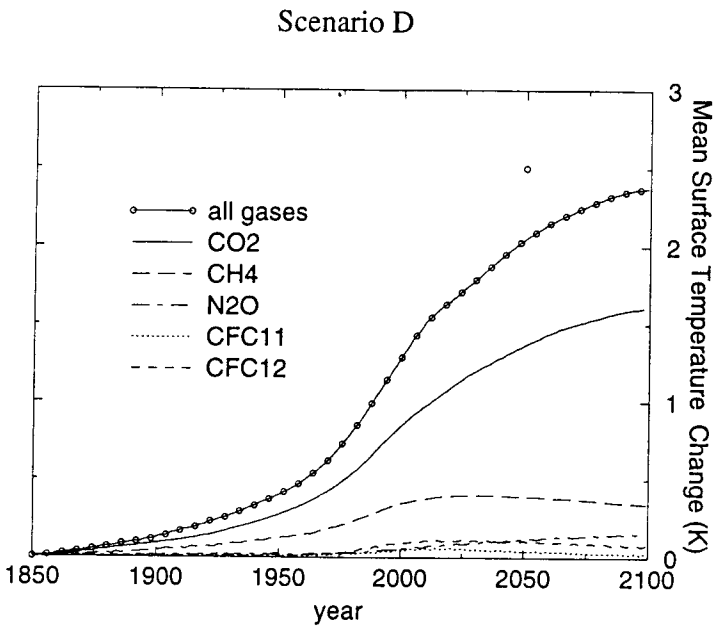

Fig. 14. Transient climate response to greenhouse gas concentration changes expressed in term of mean temperature change from 1850 (T_{1850}=287.5 K). Scenario D. The isolated little circle indicates the equilibrium response in 2050.

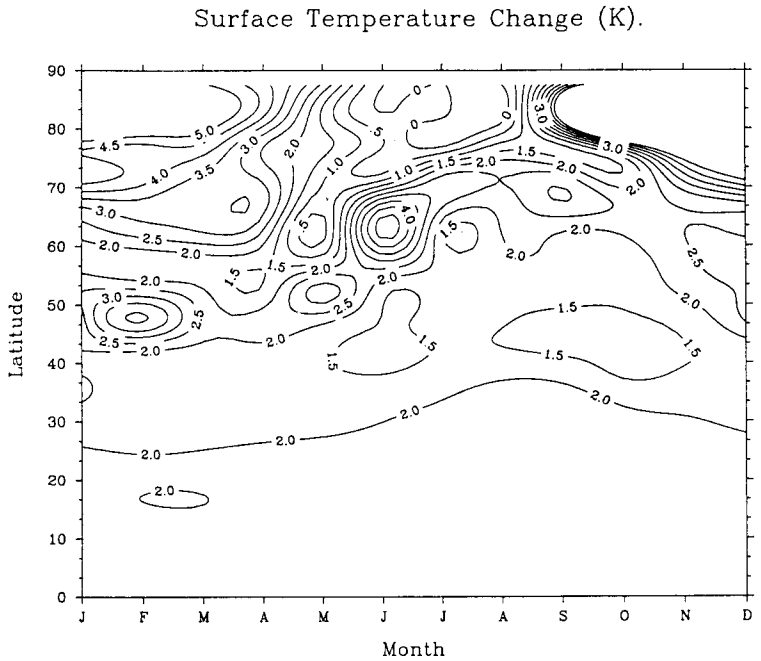

Fig. 15. Latitudinal and seasonal distribution of the temperature change between 1990 and 2050 in the transient climate simulation. Scenario BaU.

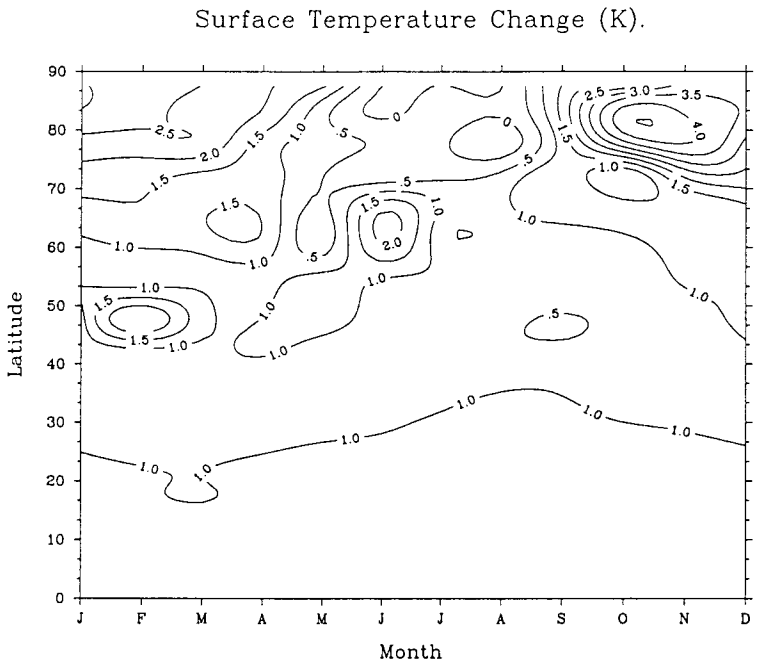

Fig. 16. Latitudinal and seasonal distribution of the temperature change between 1990 and 2050 in the transient climate simulation. Scenario D.

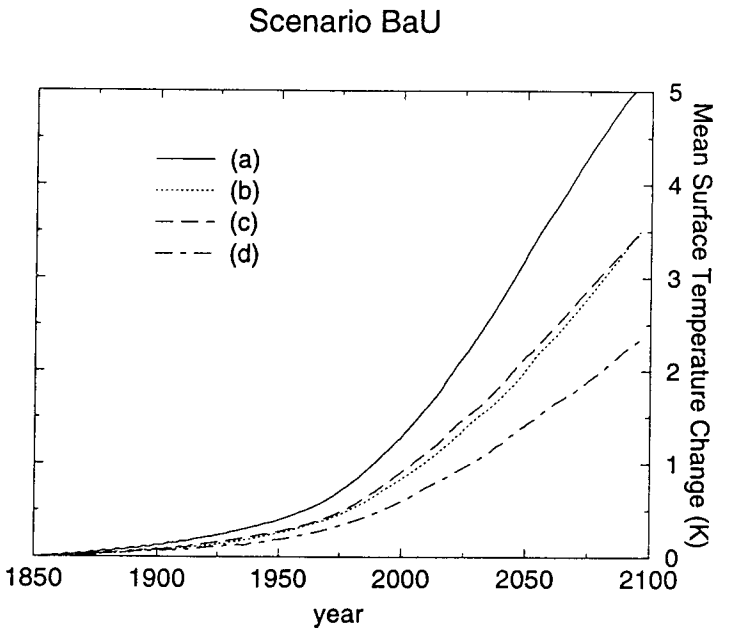

Fig. 17. Transient climate response obtained for different radiative forcing: (a) with the radiative forcing (r.f.) correction and an effective CO_2, (b) with the r.f. correction and CO_2 alone, (c) without r.f. correction and with an effective CO_2, (d) without r.f. correction and with CO_2 alone. Scenario BaU.

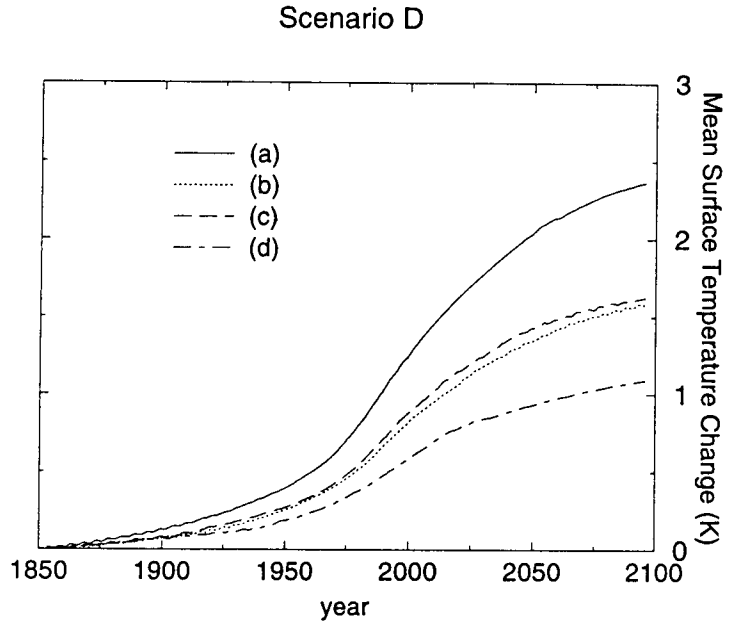

Fig. 18. Same as Figure 17 for scenario D.

The effect of the tropopause pressure parameterization on the transient climate simulations has also been evaluated. Figure 19 shows the temperature evolution obtained by using different tropopause parameterizations : the Sellers parameterization, a fixed tropopause pressure and the parameterization (9) derived from Rennick (1977). Again, it appears that the effect of the tropopause parameterization is not negligible. The largest sensitivity is obtained with the

parameterization of Rennick (1977) and the smallest with a fixed tropopause pressure. For scenario BaU, the mean temperature simulated in 2100 using these two parameterizations differs by about 1.5 K. This value is close to the difference between scenarios BaU and D for the mean temperature obtained in 2100 using a fixed tropopause pressure (about 2 K). For the standard transient simulation using the parameterization of Sellers, the latitudinal and seasonal distribution of the temperature change between 1990 and 2050 are presented in Figures 15 and 16. The difference between these temperature change distributions and those obtained with the two other tropopause parameterizations are shown in Figures 20a and 20b for scenario BaU. Results obtained for scenario D are quite similar. The effect of the tropopause parameterization is more pronounced in the high latitudes, especially during the fall and the winter.

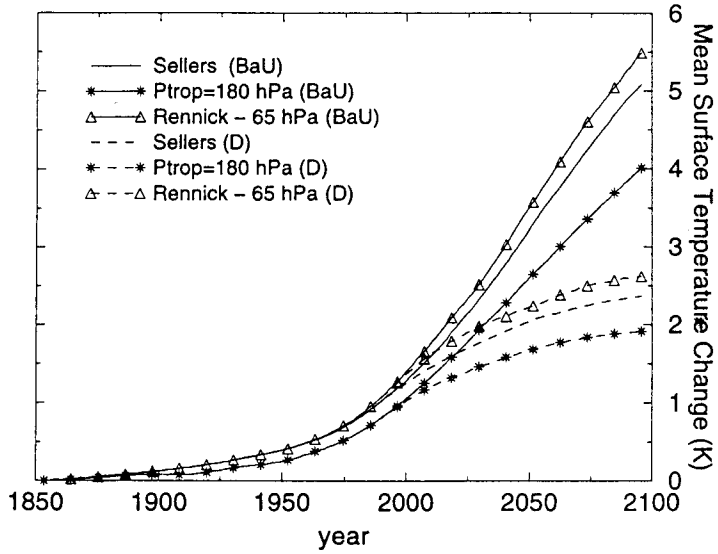

Fig. 19. Transient climate response obtained for different tropopause pressure parameterizations and for scenarios BaU and D.

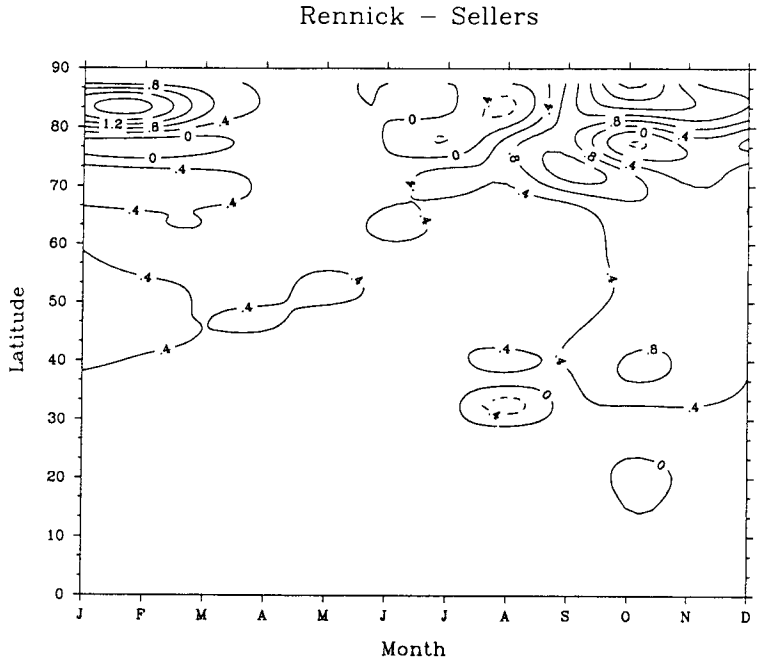

Figure 20a

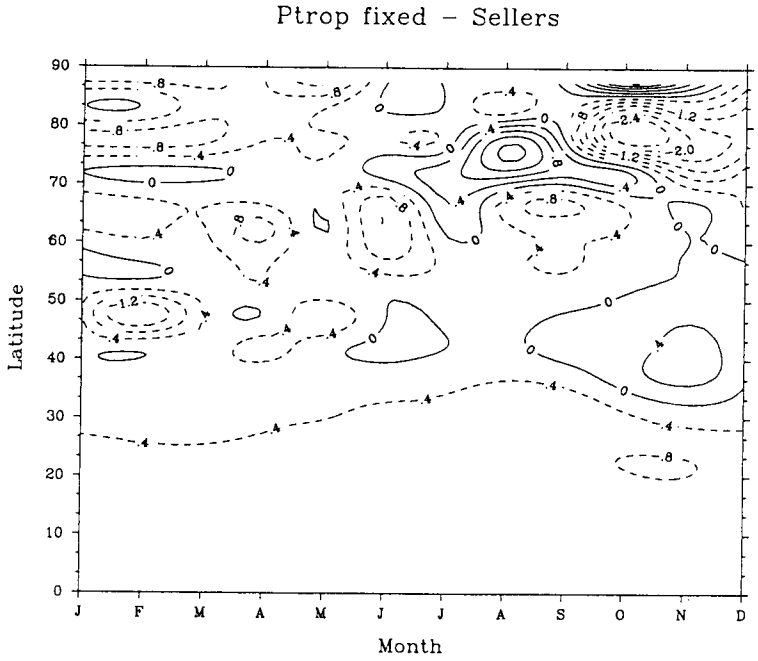

Fig. 20. Effect of tropopause parameterization on the latitudinal and seasonal distribution of the temperature (in K) change between 1990 and 2050 in the transient climate simulation using scenario BaU. (a) Difference between the results obtained using Rennick and Sellers parameterization. (b) Difference between the results obtained using a fixed tropopause pressure and the parameterization of Sellers.

6. Conclusions

A zonally averaged climate model (LLN-2D climate model) has been used to investigate the transient climate response to the anthropogenic increase of greenhouse gas concentrations. The atmospheric dynamics being represented by a two-layer quasigeostrophic model, it is impossible to distinguish between radiative forcing at the tropopause and at the top of the atmosphere. A simple method is proposed to improve the radiative forcing in atmospheric models whose dynamical processes are described with a low vertical resolution. In the LLN-2D model, this improvement increases the 2 × CO_2 climate sensitivity from 1.9 to 3 K. The radiative effects of trace gases other than CO_2 are taken into account by effective CO_2 concentrations which have been evaluated with the radiative forcing expressions given in the IPCC (1990). The radiative forcing at the tropopause obtained by this way are very similar to those obtained with radiative models including explicitly the effect of greenhouse gases other than CO_2. In a model whose aim is not to reproduce accurately the regional and vertical patterns of climate change, the effective CO_2 method proves to be quite valid.

The sensitivities of current global climate models are strongly influenced by some parameterizations. Here, we have investigated the effect of the tropopause pressure parameterization in the LLN-2D model. We have shown that small changes in tropopause pressure can induce a significant feedback in the climate system. For a CO_2 doubling these changes amount to about 10 hPa, which is much smaller than the vertical resolution of current GCMs around the tropopause. In the LLN-2D model, the climate sensitivity to a CO_2 doubling decreases by 0.7 K if this feedback is suppressed by fixing the tropopause pressures to the current values. Moreover, a large number of transient simulations over a time period extending from 1850 to 2100 have been

performed. Transient response has been simulated for both scenarios BaU (Business-as-Usual) and D (Accelerated Policies) and by considering the separate effects of the different greenhouse gases. Their joint effect has also been evaluated and the results show global warmings of 4.1 and 1.3 K respectively for scenario BaU and D between 1990 and 2100, in the standard version of the model whose 2 × CO_2 sensitivity is 3 K (including radiative forcing correction and tropopause-height feedback following Sellers (1983)). By using several tropopause parameterizations, we have further shown that these results are highly sensitive to the representation of the tropopause-height feedback. Besides, this feedback potentially influence other processes in the atmosphere, e.g. cloudiness around the tropopause, which can also affect significantly the climate sensitivity. Further refinements in the representation of these processes are thus necessary to reduce the sensitivity ranges of current climate models.

Acknowledgments

This research is supported by the EV5V-CT92-0123 and ENV4-CT95-0102 contracts with the Commission of the European Union.

REFERENCES

Berger, A., 1978. Long-term variations of daily insolation and Quaternary climatic changes. *J. Atmos. Sci.*, **35**, 2362-2367.

Berlyand, T. G., L. A. Strokina, and L. Y. E. Greshnikova, 1980. Zonal cloud distribution on the Earth. *Meteorol. Gidrol.*, **3**, 15-23.

Briegleb, B. P., 1992. Longwave Band Model for Thermal Radiation in Climate Studies. *J. Geophys. Res.*, **97**, 11475-11485.

Cess, R. D., G. L. Potter, J. P. Blanchet, G. J. Boer, A. D. Del Genio, M. Déqué, V. Dymnikov, V. Galin, W. L. Gates, S. J. Ghan, J. T. Kiehl, A. A Lacis, H. Le Treut, Z.-X. Li, X.-Z. Liang, B. J. Mc Avaney, V. P. Meleshko, J. F. B. Mitchell, J. -J. Morcrette, D. A. Randall, L. Rikus, E. Roeckner, J. F. Royer, U. Schlese, D. A. Sheinin, A. Slingo, A. P. Sokolov, K. E. Taylor, W. M., Washington, R. T.Wetherald, I. Yagai, and M. -H. Zhang, 1990. Intercomparison and Interpretation of Climate Feedbacks Processes in 19 Atmospheric General Circulation Models. *J. Geophys. Res.*, **95**, 16601-16615.

Chou, S. H., R. J. Curran, and G. Ohring, 1981. The effects of surface evaporation parametrization on climate sensitivity to solar constant variations. *J. Atmos. Sci.*, **38**, 931–938.

Colman, R. A., B. J. Mc Avaney, J. R. Fraser, L. J. Rikus, and R. R. Dahni, 1994. Snow and cloud feedbacks modelled by an atmospheric general circulation model. *Climate Dynamics*, **9**, 253-265.

Fouquart, Y., and B. Bonnel, 1980. Computations of solar heating of the Earth's atmosphere: a new parameterization. *Beitr. Phys. Atmosph.*, **53**, 35–62.

Gallée, H., J. P. van Ypersele, Th. Fichefet, Ch. Tricot, and A. Berger, 1991. Simulation of the last glacial cycle by a coupled 2-D climate-ice sheet model. Part (1): The climate model. *J. Geophys. Res., 96*, 13,139–13,161.

Gallée, H., J. P. van Ypersele, Th. Fichefet, I. Marsiat, C. Tricot, and A. Berger, 1992. Simulation of the last glacial cycle by a coupled, sectorially averaged climate–ice-sheet model.

Part 2. Response to insolation and CO_2 variation. *J. Geophys. Res.*, **97**, 15,713-15,739.

IPCC, Intergovernmental Panel on Climate Change, 1990. Climate Change. The IPCC scientific assessment. Report of Working Group 1, J. T. Houghton, C. J. Jenkins and J. J. Ephraums (eds), University Press, Cambridge, 365pp.

IPCC, Intergovernmental Panel on Climate Change, 1992. Climate Change 1992: The supplementary report to the IPCC scientific assesment. J. T. Houghton, B. A. Callander, and S. K. Varney (eds), University Press, Cambridge, 200 pp.

Kratz, D. P., M. D. Chou, and M. M-H. Yan, 1993. Infrared radiation parameterizations for the minor CO_2 bands in the window region. *J. Climate,* **6**, 1269-1281.

Lacis, A. A., and J. E. Hansen, 1974. A parameterization for the absorption of solar radiation in the Earth's atmosphere. *J. Atmos. Sci.*, **31**, 118-134.

London, J., 1957. A study of atmospheric heat balance. Report AFCRC-TR-57-287, Air Force Geophysics Lab., Hansem Field, MA 01731, USA.

Morcrette, J. J., 1984. Sur la paramétrisation du rayonnement dans les modèles de la circulation générale atmosphérique. Thèse de Doctorat d'Etat, 373 pp., Univ. des Sci. et Tech. de Lille, Lille, France.

Ohring, G. S. and Adler, 1978. Some experiments with a zonally averaged climate model. *J. Atmos. Sci.*, **35**, 186-205.

Oort, H. H., 1983. Global atmospheric circulation statistics 1958-1973, NOAA Prof. Pap. 14, 180 pp, Natl. Oceanogr. and Atmos. Admin., Washington, D.C.

Ramanathan, V., R. J. Cicerone, H. B. Singh, and J. T. Kiehl, 1985. Trace gas trends and their potential role in climate change, *J. Geophys. Res.*, **90**, 5547-5566.

Ramanathan, V., L. Callis, R. Cess, J. Hansen, I. Isaksen, W. Kuhn, A. Lacis, F. Luther, J. Mahlman; R. Reck., and M. Schlesinger, 1987. Climate-chemical interactions and effects of changing atmospheric trace gases. *Rev. Geophysics*, **25**, 1441-1482.

Rennick, M.A., 1977. The parameterization of tropospheric lapse rates in terms of surface temperature. *J. Atmos. Sci.*, **34**, 854-862.

Rind, D. and A. Lacis, 1993. The role of the stratosphere in climate change. *Surveys in Geophysics,* **14**, 133-165.

Sellers, W. D., 1983. A quasi-three-dimensional climate model. *J. Clim. Appl. Meteor.*, **22**, 1557-1574.

Sinha, A., and K. P. Shine, 1994. A One-Dimensional Study of Possible Cirrus Cloud Feedback. *J. Climate,* **7**, 158-173.

Smith, W. L., 1966. Note on the relationship between total precipitable water and surface dew point. *J. Appl. Meteor.,* **5**, 726-727.

Smits, I., Th. Fichefet, Ch. Tricot, and J. P. van Ypersele, 1993. A model study of the time evolution of climate at the secular time scale. *Atmosfera,* **6**, 255-272.

Tricot, Ch., and A. Berger, 1987. Modelling the equilibrium and transient responses of global temperature to past and future trace gas concentrations, *Climate Dynamics,* **2**, 39-61.

Van Heuklon, T. K., 1979. Estimating atmospheric ozone for solar radiation models, *Sol. Energ.,* **22**, 63-68.

Wang, W. C., M. P. Dudek, X-Z. Liang, and J. T. Kiehl, 1991. Inadequacy of effective CO_2 as a proxy in simulating the greenhouse effect of other radiatively active gases. *Nature,* **350**, 573-577.

Wang, W. C., M. P. Dudek, and X. Z. Liang, 1992. Inadequacy of effective CO_2 as a proxy in assessing the regional climate change due to other radiatively active gases. *Geophys. Res. Lett.*, **19**, 1375-1378.

World Climate Programme, 1986. A preliminary cloudless standard atmosphere for radiation computation, WCP-112, WMO/TD-No. 24, World Meteorological Organization, Geneva.